

Battery Integrated Solar Photovoltaic Energy Management System for Micro-Grid

Kannan Thirugnanam*, *Member, IEEE*, See Gim Kerk†, *Member, IEEE*, Chau Yuen*, *Senior Member, IEEE* and Balasubramaniam Thirunavukarasu*

* Engineering Product Development Pillar, SUTD, Singapore 487372 (Email:{kannan, yuenchau}@sutd.edu.sg and bs.thirunavukarasu@gmail.com).

† Power Automation, Singapore (Email: sgkerk@pa.com.sg).

Abstract—This paper proposes a battery energy management system (BEMS) for photovoltaic (PV) powered micro-grid, where the system would like to reduce the operational time of diesel generator (DG). Due to fast variations in the solar irradiance, the BEMS need to smooth the PV power fluctuations. Hence, an energy storage system is required to mitigate the PV power fluctuations. Novelty of this BEMS is to manage multiple types of batteries to reduce DG run time while extend batteries life time by controlling the batteries charge/discharge rate. The control methodology will keep the batteries charge/discharge rate within the safety limit. The proposed BEMS for micro-grid has seven modes of operation based on batteries state-of-charge, dynamic behavior of the load power, and PV power. Practical data have been used to verify the functionality of the developed BEMS for micro-grid. The performance of the proposed BEMS has been tested through the MATLAB/Simulink software.

Keywords—Battery, diesel generator, energy management system, micro-grid and photovoltaic systems.

I. INTRODUCTION

THE increasing fossil fuel price and advancement of renewable energy sources, such as photovoltaic (PV), wind, biomass, etc., are the major reasons for the development of micro-grid. Also, it's facing considerable attention in recent years to supply electricity to end users [1]–[4]. The PV power generation is expected to become a foremost energy sources for the next decade [5], [6]. Therefore, the integration of PV power into micro-grid is a viable source for electricity.

The micro-grid system is much popular to supply reliable electricity to end users, and reduce the fossil fuel consumption and greenhouse gas emissions [2], [5]. But supplying reliable power to consumer is a challenging task due to intermittent nature of PV power generation. Such fluctuations in the PV power, dynamic behavior of load power, and increasing fossil fuel price may cause several challenges to micro-grid system operators. Therefore, analysis of the impacts of PV integration in the micro-grid and solutions are needed to address the intermittent nature of PV power. Hence, an alternative solution is required to eliminate the irregular and stochastic output variations of the PV power, while reducing the DG usage. In this context, an appropriate multiple types of batteries would be a reasonable solution to solve the above problem caused by intermittent PV power, DGs utilization, and random behavior of local loads. In addition, frequent charging/discharging of the batteries are mandatory to remove the intermittent PV power and also improper charging/discharging rates could reduce the life time of the batteries. Moreover, mismanagement in energy dispatch of batteries might increase the dependency of the DGs, which increases the cost of power generation. Therefore, an battery energy management system (BEMS) for

micro-grid and control strategy is required to solve above issues.

Novelty of this proposed work is to use multiple types of batteries to reduce the DGs run time, to remove the PV power fluctuations, and to increase the batteries life time by controlling the batteries charge/discharge rate. In the literature, several methods are proposed to mitigate the PV power fluctuations, battery charge/discharge rate control, and minimize fuel consumption of DGs for the stand-alone system. These strategies are primarily grouped in to four categories. In the first approach, dynamic demand response using distributed energy resource management [6]–[8]. They are scheduling the available energy based the optimization methods to reduce the power demand of the typical distribution network or stand-alone system. This method significantly decreases the peak load demand, and mitigates transformer overloading and heating concerns.

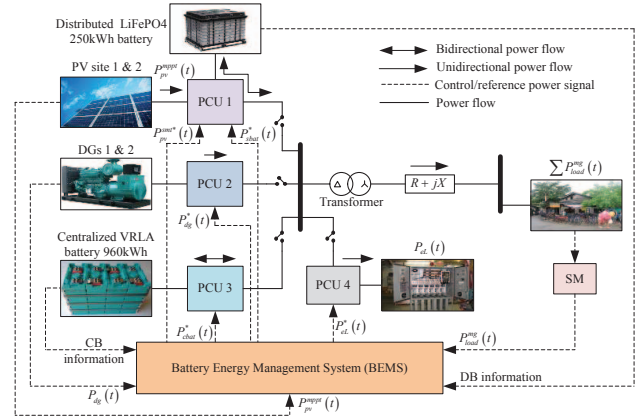


Fig. 1: Block diagram of the proposed BEMS for micro-grid.

In the second approach, the fluctuations in the PV power has been removed with battery and/or ultra-capacitors [1], [2], [9], [10]. In this method, the energy management algorithm has been developed to mitigate the PV power fluctuations, and dynamically control the battery charge/discharge rate. Also, the excess amount of the renewable energy has been stored in the battery during irradiance hours. Then the stored energy has been utilized in the peak or late night hours. The centralized and decentralized energy management system for the micro-grid has been discussed in the third approach [11], [12]. This method, fast response from energy storage device is necessary to cover the shortfall or overflow of generation due to sudden variations in the intermittent nature. Finally, energy management system has been designed to completely 'ON' or 'OFF' the grid and capable of supplying electricity to end users with the help of micro-grid [13], [14]. For example, by charging/discharging the battery during the irradiance hours,

the methods are ignores the battery state-of-charge (SOC) constraints and limitations in the charge/discharge rates, which causes the batteries life time. Also, many algorithms still do not use real-time electricity dispatch to the end users and rendering the method inapplicable. Furthermore, none of the energy management algorithm has been developed with multiple types of batteries to mitigate the PV power fluctuations, reduction in run time of DGs, and increase the battery life time by controlling the batteries charge/discharge rate. In this work, we will focus energy management algorithms for the multiple types of batteries to address: intermittency of solar power by designing a suitable charge/discharge mechanism, and energy dispatching while the use of DGs can be kept at minimum.

The block diagram of the proposed micro-grid is shown in Fig. 1. Here, * indicating the reference power signal to DGs, PV system, and multiple type of batteries. This system consists of two diesel generators (DGs), multiple power control unit (PCU1, PUC2, PUC3 and PUC4), PV systems (site 1 and 2), multiple types of batteries (distributed battery (DB) and centralized battery (CB)), local load demand ($P_{load}^{mg}(t)$), and emergency controlled load ($P_{eL}(t)$). The smart meter is used to measure the load power demand, which is input to BEMS with the delay of 1 seconds. The fluctuated maximum power ($P_{pv}^{mpp}(t)$) extracted from PV system is smoothed by using DB. This could drawn/inject the power based the smoothed reference power signal ($P_{pv}^{sm}* (t)$). If the $P_{pv}^{mpp}(t)$ is greater than $P_{pv}^{sm}* (t)$, then the DB store the excess amount of energy. Otherwise, it will supply power to regulate the PV power. The PV system and DB are connected to the PCU1, which perform maximum power point tracking (mppt), smoothing the PV power, dc/dc, and dc/ac conversion. Similarly, PCU2, PCU3 and PCU4 perform the power control of DGs, CB and emergency load via ac/dc, dc/dc, and dc/ac conversion, respectively. If the PV power generation exceeds the $P_{load}^{mg}(t)$, then the $P_{eL}(t)$ is controlled based the excess amount of power. In addition, a control strategy has been developed to control the battery charge/discharge rate within the limits.

The rest of the paper is organized as follows. Section II presents the system level modeling. The problem formulation of the micro-grid system is presented in Section III, followed by the detailed discussion about PV power mitigation, BEMS and charge/discharge rate control for multiple types of batteries are presented in Section IV. The result and discussion with the possible case study of the proposed micro-grid is presented in Section V. Finally, the conclusion is given in Section VI.

II. SYSTEM LEVEL MODELING AND DESCRIPTION

This section presents the system level modeling of typical micro-grid system layout, solar PV system, multiple types of batteries, diesel generators and PCU efficiency model.

A. Micro-grid System Model

The single line diagram of proposed micro-grid system is shown in Fig. 2. The DGs are major source for electricity and the rated capacity of 100kVA and 80kVA, respectively. The PV system consists of 12 strings of 11 panels with rated peak power capacity ($P_{pv_site1}^{rated}$) of 39.6kW_p at site 1 and 6 strings of 10 panels with rated peak power capacity ($P_{pv_site2}^{rated}$) of 18kW_p at site 2, and multiple types of batteries, such as distributed and centralized battery. This micro-grid system has 4 over-grounded boxes with smart meter, which measure the load demand.

B. Real Time PV Model

The PV cell model used in this work is shown in Fig. 3. The total amount of solar irradiance ($G(t)$) at ground surface is given in Eq. (1) [15].

$$G(t) = R_d(t) + R_{db}(t) + R_{dr}(t) \quad (1)$$

In general, the photovoltaic current ($I_{ph}(t)$) varies with respect to $G(t)$ and cell temperature ($T_c(t)$), which is given in Eq. (2).

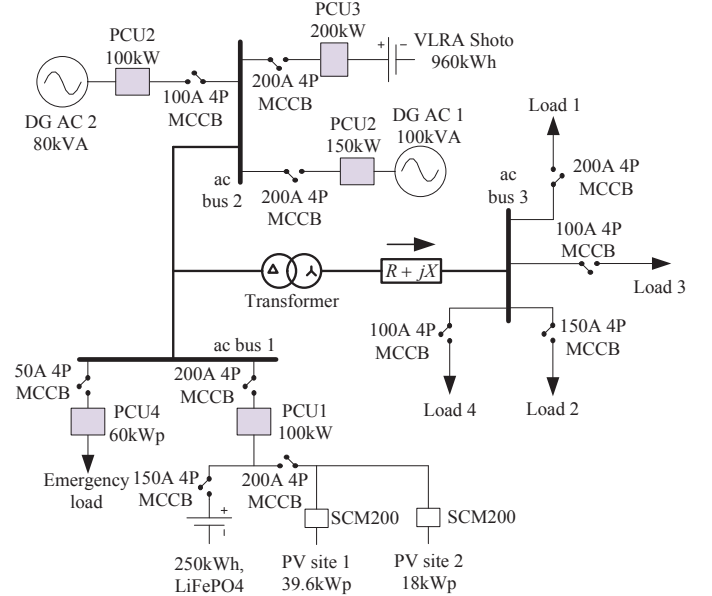


Fig. 2: Single line diagram of proposed micro-grid system.

$$I_{ph}(t) = I_{sc}(t) + k_i(T_c(t) - T_{ref}) \frac{G(t)}{G_{STC}} \quad (2)$$

where, $I_{sc}(t)$ is the short-circuit current (A), k_i is the temperature coefficient corresponding to $I_{sc}(t)$ and G_{STC} is the solar irradiance under standard-test condition. The PV cell current ($I_{pv}(t)$) obtained from Eq. (3).

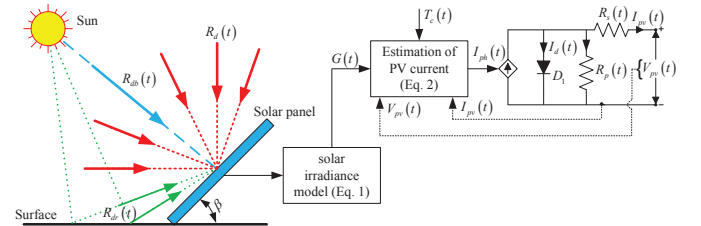


Fig. 3: Equivalent circuit of the Photovoltaic cell.

$$I_{pv}(t) = C_{np}I_{ph}(t) - C_{np}I_o(t) \left(e^{\frac{qV_{pv}(t)}{C_{ns}NkT_c}} - 1 \right) - \frac{V_{pv}(t) + I_{pv}(t)R_s}{R_p} \quad (3)$$

where, $V_{pv}(t)$ is the terminals voltage (V), $I_o(t)$ is the diode reverse saturation current (A) which depending $T_c(t)$, q is the electron charge (1.602×10^{-19} Coulomb), k is the Boltzmann's constant ($1.381 \times 10^{-23} \frac{J}{K}$), N is the diode quality factor, and C_{ns}, C_{np} are the number of PV cells connected in series and parallel. The maximum PV power extracted by using maximum power point tracking algorithm ($P_{pv}^{mpp}(t)$) can be calculated from Eq. (4).

$$P_{pv}^{mpp}(t) = V_{pv}(t) \times I_{pv}(t) \quad (4)$$

The detailed modeling of the PV can be found in [15], [16]. The parameter specifications of the PV system for site 1 and site 2 are given in Table I.

C. Battery Model

In this work, distributed battery with rated capacity of 250kWh and centralized battery with rated capacity of 960kWh battery models are developed based on the Tremblay model, which is available in the MATLAB/Simulink environment. An simple controlled voltage source connected series with internal resistance [5]. The open-circuit voltage is estimated with non-linear equation and present state-of-charge ($PSOC_{bat}(t)$) of the battery is derived from the actual battery charge/discharge current and initial state ($SOC_{ini}(t)$) of the battery. The battery characteristics are obtained from Eq. (5).

$$V_{bat}(t) = V_o(t) - k \frac{Q_{bat}(t)}{Q_{bat}(t) - \int I_{bat}(t) dt} + A \cdot \exp\left(-B \int I_{bat}(t) dt\right) \quad (5)$$

TABLE I: Specifications of the PV system.

Index	Description	PV cell specifications	
Whole system at site 1	12 string of 11 panels	I_{sc} (A), V_{oc} (V)	8.68, 0.632
Whole system at site 2	6 strings of 10 panels	Maximum peak current, I_{mp} (A)	8.04
Every single panel	72 cells are in series	Maximum peak voltage, V_{mp} (V)	0.51
Single panel open-circuit voltage, V_{oc} (V)	45.5	C_{ns}	72
Single panel short circuit current, I_{sc} (A)	8.68	C_{np}	1
Each solar panel power (Wp)	300	Each cell power (Wp)	4.166

where, $V_{bat}(t)$, $V_o(t)$ are the battery terminal voltage under no-load condition and battery constant voltage (V), $Q_{bat}(t)$ is the battery capacity (Ah), $I_{bat}(t)$ is the battery current (A), k is polarization voltage (V), A is the exponential voltage (V), and B is the exponential battery capacity (Ah^{-1}). The $PSOC_{bat}(t)$ of the battery can be calculated from Eq. (6).

$$PSOC_{bat}(t) = SOC_{ini}(t) \pm \frac{I_{bat}(t) \times \Delta t}{Q_{bat} \times 3600} \quad (6)$$

where, Δt is the changing time and \pm indicate battery charging or discharging. Available energy ($E_{bat}^{avil}(t)$) to supply at any time instant can be calculated from Eq. (7).

$$E_{bat}^{avil}(t) = Q_{bat}(t) V_{bat}(t) PSOC_{bat}(t) \quad (7)$$

The required energy ($E_{bat}^{req}(t)$) to store into the battery can be calculated from Eq. (8).

$$E_{bat}^{req}(t) = E_{bat}^{rated} - E_{bat}^{avil}(t) \quad (8)$$

where, E_{bat}^{rated} is the rated capacity of the battery. Due to simple and easy implementation, the MATLAB/Simulink model is commonly used for simulation studies. The CB and DB characteristics are obtained by tuning the battery parameters.

D. Diesel Generator Model

In the existing system, the DGs are the major source for electricity. Hence, a system level mathematical model is developed. Normally, the DG are connected in parallel to maintain the ac bus voltage equal to the generator output voltage. Two diesel generators (DGs) are used with nominal

rated capacity (P_{dg1}^{rated} , P_{dg2}^{rated}) of 100kVA and 80kVA, respectively. In this work, the DGs are considered as a backup energy source, when there is no PV power generation and/or energy status of the batteries are less than the requirement. If the $PSOC_{bat}(t)$ is reached to minimum SOC (SOC_{bat}^{min}) limit, then the DGs supply required energy. The DGs output voltage ($V_{dg}(t)$) is constant. Therefore, average DGs power ($P_{dg}(t) = P_{dg1}(t) + P_{dg2}(t)$) depends the maximum nominal DGs current ($I_{dg}^{max}(t)$) and output decision variable (X_{dg}).

$$P_{dg}(t) = \sqrt{3} V_{dg}(t) I_{dg}^{max}(t) X_{dg} \quad (9)$$

The fuel consumption (FC_{dg}) of DG varies with respect to type of generator, size and manufacturer. In general, the rated fuel consumption of DG (DG_{rfc}) depends the efficiency or heat rate of the generator and heat content of the fuel. The DG_{rfc} varies from 0.32 to 0.53 l/kWh [17], [18]. However, the fuel consumption of the DG can be modeled in terms of energy supplied to consumers, which is given in Eq. (10).

$$E_{dg}(t) = \sum_{d=1}^n P_{dg}(t) \Delta t_d, \quad \forall n = 1, 2, 3, \dots \quad (10)$$

where, d is the number of days. The mathematical expression for fuel consumption of DG (FC_{dg}) is given in Eq. (11).

$$FC_{dg} = DG_{rfc} \times E_{dg}(t) \quad (11)$$

E. Efficiency Model of i^{th} Power Control Unit

The i^{th} power control unit (PCU) is modeled based the polynomial equation with coefficients, which is given in Eq. (12). The coefficients are tuned manually to obtained the error tolerance is less than 3% – 6%.

$$\eta_{PCU,i}(\%) = 100 - \frac{1}{x_i} (k_1 + k_2 x_i + k_3 x_i^2 + k_4 x_i^3) \quad (12)$$

where, x_i is the ratio between i^{th} PCU input power and rated power, and k_1 , k_2 , k_3 , k_4 are the polynomial coefficients.

III. PROBLEM FORMULATION

The single line diagram of micro-grid system is shown in Fig. 2. The micro-grid sources (DGs, PV system, and multiple types of batteries) are connected in ac bus 1 and 2 and loads are connected in ac bus 3. The DB would regulate the PV power fluctuations during sunshine hours and discharge the energy in late-night/morning hours based on $PSOC_{dbat}(t)$ levels. Also, the CB charge/discharge their energy with respect to PV power generation, $PSOC_{cbat}(t)$ and load demand. The net power ($P_{net}^{mg}(t)$) of the micro-grid can be obtained from Eq. (13).

$$P_{net}^{mg}(t) = P_{pv}^{smi}(t) + P_{dg}(t) \pm P_{bat}(t) - P_{load}^{mg}(t) \quad (13)$$

where, $P_{pv}^{smi}(t)$ is the smoothed PV power ($P_{pv}^{smi}(t) = P_{pv,site1}^{mpp}(t) + P_{pv,site2}^{mpp}(t)$), $P_{dg}(t)$ is the average DGs power ($P_{dg}(t) = P_{dg1}(t) + P_{dg2}(t)$), $P_{load}^{mg}(t)$ is the micro-grid load power ($P_{load}^{mg}(t) = P_{load1}(t) + P_{load2}(t) + P_{load3}(t) + P_{load4}(t)$), $P_{bat}(t)$ is the injected/absorbed power of CB and DB ($P_{bat}(t) = \pm P_{cbat}(t) \pm P_{dbat}(t)$). In Eq. (13), the \pm sign indicate the battery is charging or discharging. The power loss ($P_{loss}^{mg}(t)$) of the micro-grid is depends on the losses due to line reactance ($R + jX$) and i^{th} PCU efficiency ($P_{loss}^{conv}(t)$), which can be obtained from Eq. (14).

$$P_{loss}^{mg}(t) = (P_{loss}^{mg}(t) + jQ_{loss}^{mg}(t)) + P_{loss}^{conv}(t) \quad (14)$$

The line reactance of the micro-grid system can be obtained from Eq. (15).

$$P_{loss}^{mg}(t) = \frac{P_{load}^{mg}(t)^2 + Q_{load}^{mg}(t)^2}{V_{ac\ bus\ 3}(t)^2} R; \quad Q_{loss}^{mg}(t) = \frac{P_{load}^{mg}(t)^2 + Q_{load}^{mg}(t)^2}{V_{ac\ bus\ 3}(t)^2} X \quad (15)$$

The objective of this proposed work is to use multiple types of batteries in micro-grid with reduction in DGs run time, remove PV power fluctuations, and increase batteries life time by controlling the batteries charge/discharge rate. This can be archived with the proper energy management system for multiple types of batteries and PV system. The objective function for reduction in DGs run time DG ($RT_{rdg}(t_{on})$) based on PV power and batteries energy is given in Eq. (16).

$$\min \left(\sum_{d=1}^n E_{dg}(t_d) \right) \times RT_{rdg}(t_{on}), \quad \forall n = 1, 2, \dots, k \quad (16)$$

$$\text{s.t.} \begin{cases} P_{pv}^{smt*}(t) \pm \frac{E_{cbat}(t) + E_{dbat}(t)}{D} \geq P_{load}^{mg}(t) + P_{loss}^{mg}(t) \\ SOC_{bat}^{\min} \leq PSOC_{cbat}(t) \leq SOC_{bat}^{\max} \\ PSOC_{dbat}(t) \geq 0.7 \times SOC_{bat}^{\max} \end{cases} \quad (17)$$

where, $E_{dg}(t)$ is the n^{th} day DGs energy and D is the duration to control the battery charge/discharge rate. The energy loss of battery is directly proportional to the charge/discharge rate and temperature. Hence, an algorithm is developed to control the D , which is explained in Section IV-C. The objective function to control the battery charge/discharge rate is given in Eq. (18).

$$\min \left(\sum_{d=1}^n \frac{I_{cbat}(t_d) \times V_{cbat}(t_d)}{E_{cbat}^{avil}(t)}, \sum_{d=1}^n \frac{I_{dbat}(t_d) \times V_{dbat}(t_d)}{E_{dbat}^{avil}(t)} \right) \quad (18)$$

$$\forall n = 1, 2, \dots, k$$

$$\text{s.t.} \begin{cases} I_{cbat}(t) \leq I_{cbat}^{\max}, \quad \forall I_{cbat}(t) \in \frac{E_{cbat}^{avil}(t)}{V_{cbat}(t) \times \Delta t} \\ I_{dbat}(t) \leq I_{dbat}^{\max}, \quad \forall I_{dbat}(t) \in \frac{E_{dbat}^{avil}(t)}{V_{dbat}(t) \times \Delta t} \\ SOC_{bat}^{\min} \leq PSOC_{cbat}(t) \leq SOC_{bat}^{\max} \\ SOC_{bat}^{\min} \leq PSOC_{dbat}(t) \leq SOC_{bat}^{\max} \end{cases} \quad (19)$$

Next Section presents the mitigation of intermittent PV power, BEMS for micro-grid with different modes of operation (MOP) to achieve the above objective function.

IV. BATTERY ENERGY MANAGEMENT SYSTEM FOR MICRO-GRID

The proposed BEMS would remove fluctuations in the PV power, reduction in DGs run time, and increase batteries life time by controlling batteries charge/discharge rate.

A. Fluctuated PV Power Mitigation

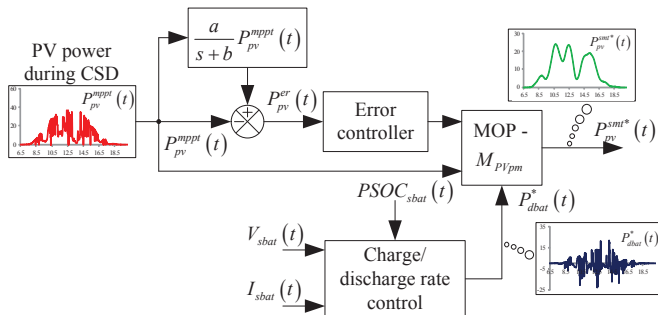


Fig. 4: PV power mitigation with distributed battery.

Fig. 4 shows the block diagram of PV power mitigation with the help of DB, which remove the PV power fluctuations. The maximum peak power extracted from PV site 1 and

2 are filtered ($P_{pv}^{fl}(t)$). The error signal ($P_{pv}^{er}(t)$) is generated by comparing $P_{pv}^{mpppt}(t)$ and $P_{pv}^{fl}(t)$. The PI error controller is used in this work to reduce the $P_{pv}^{er}(t)$. The controller gains are tuned manually to get the desired smoothed PV power output. The DB would charge/discharge based on the PV power with respect to MOP-5, which is given in Table II.

B. Modes of Operation

TABLE II: Modes of operations (MOP) for the proposed BEMS (1 - normal mode, 2 - excess energy mode, 3 - energy deficit mode, 4 - battery energy mode, 5 - PV power mitigation mode, 6 - emergency load mode, and 7 - battery charging mode).

MOP	Conditions	Actions
1	$P_{pv}^{smt*}(t) = P_{pv}^{\min}$ $E_{cbat}(t) = 0, E_{dbat}(t) = 0$	$P_{dg}^*(t) = P_{dem}^{mg}(t)$
2	$P_{pv}^{smt*}(t) \geq P_{dem}^{mg}(t)$ $SOC_{bat}^{\min} \leq PSOC_{cbat}(t) \leq SOC_{bat}^{\max}$	$P_{cbat}^*(t) = \frac{(P_{pv}^{smt*}(t) - P_{dem}^{mg}(t)) \times E_{cbat}^{req}(t)}{D}$ $P_{pv}^{smt*}(t) = P_{dem}^{mg}(t) - P_{cbat}^*(t)$
3	$P_{pv}^{smt*}(t) \leq P_{dem}^{mg}(t)$ $SOC_{bat}^{\min} \leq PSOC_{cbat}(t) \leq SOC_{bat}^{\max}$	$P_{pv}^*(t) = P_{dem}^{mg}(t)$ $P_{cbat}^*(t) = \frac{(P_{pv}^{smt*}(t) - P_{dem}^{mg}(t)) \times E_{cbat}^{avil}(t)}{D}$
	$P_{pv}^{smt*}(t) \leq P_{dem}^{mg}(t)$ $PSOC_{cbat}(t) \leq SOC_{bat}^{\min}$	$P_{pv}^*(t) = P_{dem}^{mg}(t)$ $P_{bat}^*(t) = \frac{E_{cbat}(t)}{D}$ $P_{dg}^*(t) = P_{bat}^*(t) + (P_{dem}^{mg}(t) - P_{pv}^*(t))$
4	$P_{pv}^{smt*}(t) \leq P_{pv}^{\min}$ $SOC_{bat}^{\min} \leq PSOC_{cbat}(t) \leq SOC_{bat}^{\max}$ $PSOC_{dbat}(t) \geq 0.7 \times SOC_{bat}^{\max}$	$P_{cbat}^*(t) + P_{dbat}^*(t) = P_{dem}^{mg}(t)$ $P_{cbat}^*(t) = \frac{P_{dem}^{mg}(t) \times E_{cbat}^{avil}(t)}{E_{cbat}^{total}}$ $P_{dbat}^*(t) = \frac{P_{dem}^{mg}(t) \times E_{dbat}^{avil}(t)}{E_{dbat}^{total}}$ $E_{bat}^{total} = E_{cbat}^{rated} + E_{dbat}^{rated}$
	$P_{pv}^{smt*}(t) \leq P_{pv}^{\min}$ $SOC_{bat}^{\min} \leq PSOC_{cbat}(t) \leq SOC_{bat}^{\max}$ $PSOC_{dbat}(t) \leq 0.7 \times SOC_{bat}^{\max}$	$P_{cbat}^*(t) = P_{dem}^{mg}(t)$ $P_{cbat}^*(t) = \frac{P_{dem}^{mg}(t) \times E_{cbat}^{avil}(t)}{E_{cbat}^{rated}}$
	$P_{pv}^{smt*}(t) \leq P_{pv}^{\min}$ $PSOC_{cbat}(t) \leq SOC_{bat}^{\min}$ $PSOC_{dbat}(t) \leq 0.7 \times SOC_{bat}^{\max}$	$P_{cbat}^*(t) = \frac{E_{cbat}(t)}{D}$ $P_{dg}^*(t) = P_{cbat}^*(t) + P_{dem}^{mg}(t)$
5	$P_{pv}^{mpppt}(t) \geq P_{pv}^{\min}$ $SOC_{bat}^{\min} \leq PSOC_{dbat}(t) \leq SOC_{bat}^{\max}$	if $P_{pv}^{mpppt}(t) \geq P_{pv}^{smt*}(t)$ $P_{dbat}^*(t) = P_{pv}^{mpppt}(t) - P_{pv}^{smt*}(t)$ else $P_{dbat}^*(t) = P_{pv}^{smt*}(t) - P_{pv}^{mpppt}(t)$ end
	$P_{pv}^{mpppt}(t) \geq P_{pv}^{\min}$ $PSOC_{dbat}(t) \leq SOC_{bat}^{\min}$	PV system stand - by mode
	$P_{pv}^{mpppt}(t) \geq P_{pv}^{\min}$ $PSOC_{dbat}(t) \geq SOC_{bat}^{\max}$	PV system stand - by mode $P_{dbat}^*(t) = \frac{P_{dem}^{mg}(t) \times E_{dbat}^{avil}(t)}{D}$
6	$P_{pv}^{smt*}(t) \geq P_{dem}^{mg}(t)$ $PSOC_{cbat}(t) \geq SOC_{bat}^{\max}$	$P_{cbat}^*(t) = 0$, Stand - by mode $P_{pv}^{smt*}(t) = P_{dem}^{mg}(t)$ $P_{el}^*(t) = P_{pv}^{smt*}(t) - P_{dem}^{mg}(t)$
7	$P_{pv}^{smt*}(t) \leq P_{pv}^{\min}$ $PSOC_{cbat}(t) \leq SOC_{bat}^{\min}$ $PSOC_{dbat}(t) \leq SOC_{bat}^{\max}$	$P_{dg}^*(t) = \frac{E_{dbat}^{req}(t)}{D} + \frac{E_{cbat}^{req}(t)}{D} + P_{dem}^{mg}(t)$

Battery energy management system is designed based on the modes of operation, which is given Table II. Here, * denoting the reference power for batteries, DGs, and PV system. For example, $P_{dg}^*(t) = 9.2kW$ and $P_{cbat}^*(t) = -12.5kW$, then the DGs and CB supply the desired power. The proposed BEMS have different mode of operations (MOP), where the summary of all operating modes are given in Table II.

The batteries and PV systems are not considered in MOP-1. The DGs power levels is controlled by adjusting the control parameters X_{dg} . In MOP-2, if the $P_{pv}^{smt*}(t)$ exceeds load demand ($P_{dem}^{mg}(t) = P_{load}^{mg}(t) + P_{loss}^{mg}(t)$), then the excess amount of energy would be stored into CB based on $PSOC_{cbat}(t)$ level. In MOP-3, there are two sub-modes with respect to battery $PSOC_{cbat}(t)$ level. If the PV power generation is less than the $P_{dem}^{mg}(t)$, then the CB would inject the available energy into micro-grid load. Due to supplying energy to micro-grid loads, the batteries SOC levels would reach to SOC_{bat}^{\min} .

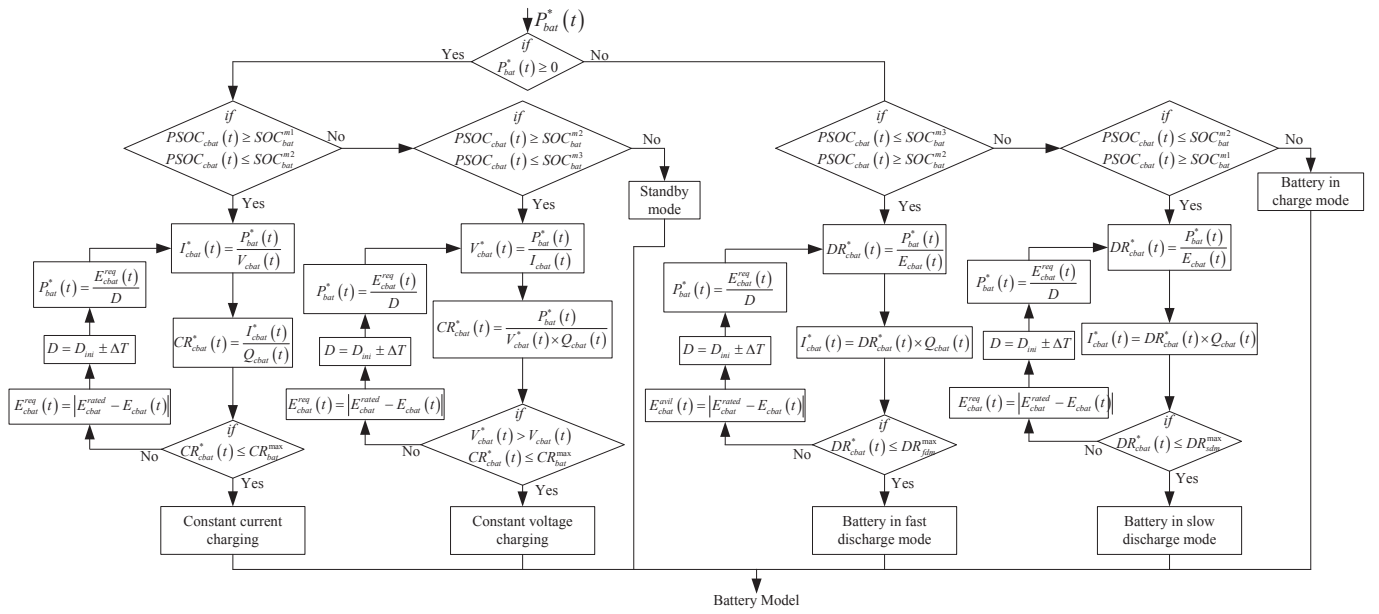


Fig. 5: Flowchart of the proposed battery charge/discharge rate control for CB.

In this situation, DGs are to provide the deficit power to loads and batteries by adjusting X_{dg} . The PV power generation falls below P_{pv}^{min} during night hours or low solar irradiance. The MOP-4 handle this situation. In this mode, there are three sub-modes with respect to $PSOC_{cbat}(t)$ and $PSOC_{dbat}(t)$. The CB and DB would discharge the available energy. If the $PSOC_{cbat}(t)$ reached to SOC_{cbat}^{min} and $PSOC_{dbat}(t)$ reached to $0.7 \times PSOC_{dbat}(t)$, then the DGs are turned 'ON' to supply electricity to local loads. The fluctuations in the PV power is removed with DB at MOP-5, which is discussed in the above section. In MOP-6, suppose the CB is fully charged ($PSOC_{cbat}(t) \geq SOC_{cbat}^{max}$) during $P_{pv}^{sm*}(t) \geq P_{dem}^{mg}(t)$, then the $P_{eL}(t)$ is turned 'ON' to consume the PV power. Finally in MOP-7, the CB and SB are charged from DGs, if the $PSOC_{cbat}(t)$ and $PSOC_{sbat}(t)$ levels are less than SOC_{cbat}^{min} and PV power generation is less than P_{pv}^{min} . The BEMS is implemented in MATLAB Simulink environment based on the constraints and MOPs are given in Table II.

C. Battery Charge/Discharge Rate Control

The batteries charge/discharge rate control algorithm chooses the minimum rate to regulate the current flows into/from the CB and DB. The minimum of the charge/discharge rate could reduce the sudden fluctuations in the battery current due to intermittent PV power. The batteries charge and discharge methodology is given in Fig. 6. The batteries are charge based on the SOC levels (SOC_{cbat}^m1 , SOC_{cbat}^m2 and SOC_{cbat}^m3). If the $PSOC_{cbat}(t)$ is less than SOC_{cbat}^m2 , then the CB is charging with constant current charging method. For discharging scenario, the control algorithm decide to discharge the battery in fast or slow mode by adjusting total duration (D) to absorb/inject energy. The flow chart for charge/discharge rate control for CB is shown in Fig. 5. Similar type of control logic has been used for DB. Also, the SOC limits (SOC_{cbat}^{min} , SOC_{cbat}^{max}) of the CB and DB are considered in this work to preventing over charge or discharge. Suppose, the DB charge rate exceeds the CR_{dbat}^{max} , the algorithm adjust the D to reduce the $CR_{dbat}(t)$.

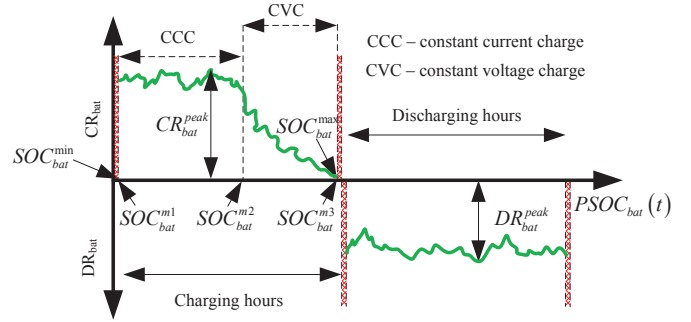


Fig. 6: Batteries charge/discharge rate control.

V. RESULTS AND DISCUSSION

The proposed BEMS for micro-grid system has been verified with real-time data four types of loads (load1, load2, load3, and load4), which is shown in Fig. 7. The loads and PV power generation data are obtained from the smart meter. Simulations are performed by considering DGs, PV system, multiple types of batteries during rainy day (RD), cloudy day (CD), cloudy&sunny day (CSD), and sunny day (SD). To study the real time situations and behavior of proposed BEMS for micro-grid, the following cases are considered:

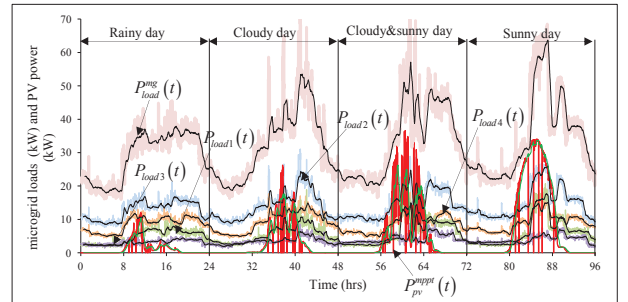


Fig. 7: Practical data of micro-grid load and total PV power during rainy (15/05/2015), cloudy (23/05/2015), cloudy&sunny (28/05/2015), and sunny (02/06/2015) days.

- Case I - The DGs supply electricity to loads at different

days.

- **Case II** - The DGs, PV system, and multiple types of batteries are supply power to loads.

During sunshine hours, battery charge/discharge rate controller decides the magnitude of current and direction of power flow depending on the PV power and oads variation. The distributed battery could not supply power to loads during PV power generation. The DGs supply electricity to loads in case I. To check the DGs run time and fossil fuel consumption, the case study has been considered. The both DGs are considered as single source for electricity, where the total power handling capacity is 180kVA. Total energy supplied from DGs, FC_{dg} per kWh, and DGs turn 'ON' time has been summarized in Table III.

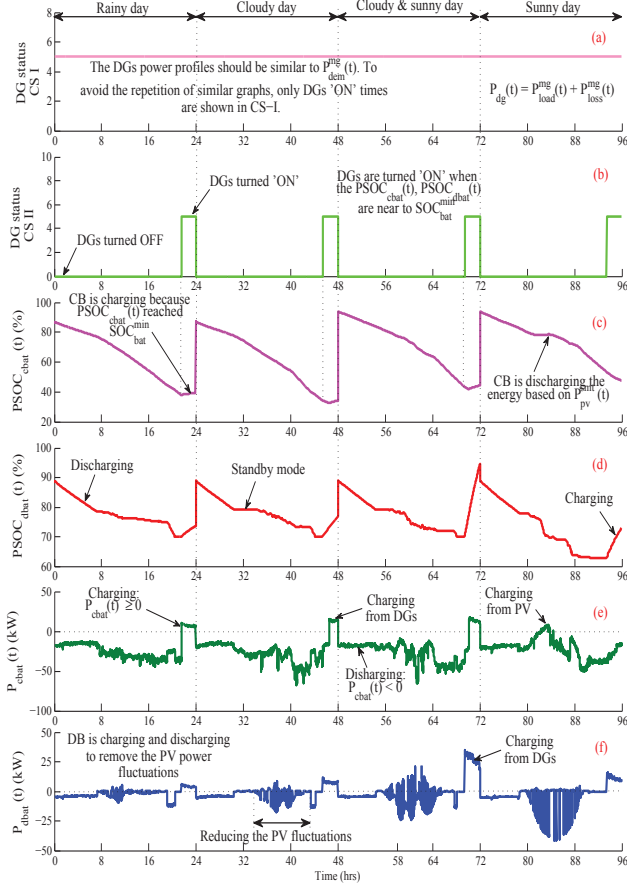


Fig. 8: Simulation results : (a) DGs status for case I (b) DGs status for case II (c) centralized battery $PSOC_{cbat}(t)$ for case II (d) distributed battery $PSOC_{dbat}(t)$ for case II (e) centralized battery power $P_{cbat}(t)$ for case II and (f) distributed battery power $P_{dbat}(t)$ for case II.

In case II, the initial values of $PSOC_{cbat}(t)$ and $PSOC_{dbat}(t)$ are chosen randomly. To show the reduction in DGs run time and PV power fluctuations, and batteries life time has been increased by controlling charge/discharge rate, this case study has been chosen. The DGs are turned 'ON', when batteries SOC levels reach to SOC_{bat}^{min} or PV power generation less than P_{pv}^{min} .

Fig. 8 - Fig. 9 shows the simulation results for case I and case II. The diesel generators status are shown in Fig. 8(a). From this figure, the DGs are turned 'ON' whole days ($4 \times 24 = 96hrs$). The DGs power should be equal to $P_{dem}^{mg}(t)$. The load profiles for different days are shown in Fig. 7. Hence, the $P_{dg}(t)$ follow the loads profile. Therefore, to avoid the

reputation of graph, the DGs powers are not shown for case I. Energy supplied from DGs (E_{dg}), total energy of the CB and DB (E_{bat}), total energy of PV system (E_{pv}), and DGs turned 'ON' status for case II has been summarized in Table III. In the RD at case I, it consumed 342.31 liters of fossil fuel to supply 729.04kWh energy to loads.

The centralized battery present SOC level is shown in Fig. 8(c). Every day, the battery initial SOC is set to high values. The $PSOC_{cbat}(t)$ is decreasing during the day time and it reach to minimum values, then the DGs are turned 'ON' to increase the SOC levels. The DGs turned 'ON' status for case II is shown in Fig. 8(b). Similarly, the $PSOC_{dbat}(t)$ is shown in Fig. 8(d), where the SOC level is continuously varying with respect to PV power. If the $PSOC_{dbat}(t)$ is greater than $0.7 \times PSOC_{bat}^{max}$ during night/morning hours, then the battery supply power to loads else the battery in standby mode.

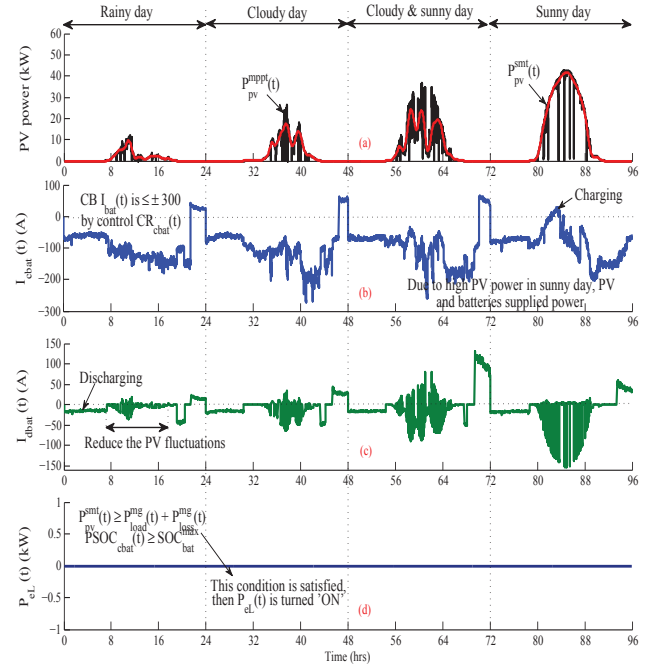


Fig. 9: Simulation results: (a) Fluctuated PV power ($P_{pv}^{mpp}(t)$) and smothering PV power ($P_{pv}^{smt}(t)$) for case II (b) centralized battery current $I_{cbat}(t)$ for case II and (c) distributed battery current $I_{dbat}(t)$ for case II and (d) emergency load power $P_{eL}(t)$.

The $P_{cbat}(t)$ and $P_{dbat}(t)$ are shown in Fig. 8(e)-(f). The batteries power is controlled by adjusting duration to supply power to loads. In RD from 00:00hrs to 07:16hrs, the CB and DB are supply power to loads. The DB is starting to charge/discharge based on the $P_{pv}^{mpp}(t)$ because PV power is greater than zero at 07:16hrs. During this time instant, the batteries are working in MOP-5 and MOP-3, respectively. At 19:06hrs, the DB is discharging the energy because the SOC level greater than 70%. The $P_{cbat}(t)$ is reduced and $P_{dbat}(t)$ is increased based on the reference signal generated from the BEMS. From 20:23hrs to 21:50hrs, the DB battery is standby mode due to SOC levels. Hence, the DGs are turned 'ON' at 21:50hrs because the $PSOC_{cbat}(t)$ and $PSOC_{dbat}(t)$ reached minimum value.

Fig. 9(a) shows the $P_{pv}^{smt}(t)$ and $P_{pv}^{mpp}(t)$. Due to rain, the power generation is very low. Normally, the DB continuously charge/discharge based on the $P_{pv}^{mpp}(t)$ and SOC levels. The frequently charging and discharging DB power is shown in Fig. 8(f). During sunshine hours, the DB reducing fluctuations in the PV power, and remaining hours, this will supply energy

TABLE III: Summy of BEMS for micro-grid during RD, CD, CSD, and SD.

Days	Case I		Case II			
	E_{dg} (kWh)	DGs 'ON' time (hrs)	E_{bat} (kWh)	E_{pv} (kwh)	E_{dgs} (kWh)	DGs 'ON' time (hrs)
RD	729.04	24	562.65	29.92	100.65	2:10
CD	802.93	24	628.04	71.63	89.99	2:04
CSD	842.61	24	546.48	122.06	162.69	2.25
SD	857.30	24	573.09	259.23	36.17	1:50

to loads or charging from DGs based on the $PSOC_{dbat}(t)$ levels. The $I_{cbat}(t)$ and $I_{dbat}(t)$ are shown in Fig. 9(b)-(c). The batteries current is controlled by tuning the charge/discharge rate. The emergency load is turned off due to low PV power generation and SOC levels, which is shown in Fig. 9(d). It is observed from Fig. 8, Fig. 9, and Table III, the proposed BEMS supply reliable electricity to consumers, reduced the DGs run time, removed the fluctuations in the PV power, and improving the battery life time by controlling the batteries charge/discharge rate.

VI. CONCLUSION

In this paper, battery energy management system (BEMS) for micro-grid system has been proposed with diesel generators, photovoltaic system, and multiple types of batteries such as centralized and distributed battery. The BEMS have different modes of operation based on the PV power generation, loads and batteries energy. The developed BEMS reduced DGs run time (fossil fuel consumption), increased the battery life time by controlling charge/discharge rate and, supplied reliable power to consumers. Fluctuations in the PV power have been reduced by charging/discharging the distributed battery energy. Also, the battery charge/discharge rate has been controlled by adjusting the duration to absorb/inject energy.

REFERENCES

- [1] C. Hill, M. Such, D. Chen, J. Gonzalez, and W. Grady, "Battery energy storage for enabling integration of distributed solar power generation," *IEEE Trans. Smart Grid*, vol. 3, no. 2, pp. 850–857, June 2012.
- [2] M. Pedrasa, T. Spooner, and I. MacGill, "Coordinated scheduling of residential distributed energy resources to optimize smart home energy services," *IEEE Trans. Smart Grid*, vol. 1, no. 2, pp. 134–143, Sept 2010.
- [3] W. Tushar, C. Yuen, S. Huang, D. Smith, and H. Poor, "Cost minimization of charging stations with photovoltaics: An approach with ev classification," *IEEE Trans. Intelligent Transportation Systems*, vol. PP, no. 99, pp. 1–14, Aug. 2015.
- [4] W. Tushar, S. Huang, C. Yuen, J. Zhang, and D. Smith, "Synthetic generation of solar states for smart grid: A multiple segment markov chain approach," pp. 1–6, Oct 2014.
- [5] S. Hakimi and S. Moghaddas-Tafreshi, "Optimal planning of a smart microgrid including demand response and intermittent renewable energy resources," *IEEE Trans. Smart Grid*, vol. 5, no. 6, pp. 2889–2900, Nov 2014.
- [6] B. Jiang and Y. Fei, "Smart home in smart microgrid: A cost-effective energy ecosystem with intelligent hierarchical agents," *IEEE Trans. Smart Grid*, vol. 6, no. 1, pp. 3–13, Jan 2015.
- [7] J. G. d. S. F. J. T. O. Yumiko Iwafune, Takashi Ikegami and K. Ogimoto, "Cooperative home energy management using batteries for a photovoltaic system considering the diversity of households," *J. Energy Conversion and Management*, vol. 96, pp. 322–329, March 2015.
- [8] K. Rahbar, J. Xu, and R. Zhang, "Real-time energy storage management for renewable integration in microgrid: An off-line optimization approach," *IEEE Trans. Smart Grid*, vol. 6, no. 1, pp. 124–134, Jan 2015.
- [9] H. Zhou, T. Bhattacharya, D. Tran, T. Siew, and A. Khambadkone, "Composite energy storage system involving battery and ultracapacitor with dynamic energy management in microgrid applications," *IEEE Trans. Power Electron.*, vol. 26, no. 3, pp. 923–930, March 2011.
- [10] S. Augustine, M. Mishra, and N. Lakshminarasamma, "Adaptive droop control strategy for load sharing and circulating current minimization in low-voltage standalone DC microgrid," *IEEE Trans. Sustain. Energy*, vol. 6, no. 1, pp. 132–141, Jan 2015.
- [11] K. Worthmann, C. Kellett, P. Braun, L. Grune, and S. Weller, "Distributed and decentralized control of residential energy systems incorporating battery storage," *IEEE Trans. Smart Grid*, vol. 6, no. 4, pp. 1914–1923, July 2015.
- [12] G. Wang, M. Ciobotaru, and V. Agelidis, "Power smoothing of large solar PV plant using hybrid energy storage," *IEEE Trans. Sustain. Energy*, vol. 5, no. 3, pp. 834–842, July 2014.
- [13] M. Alam, K. Muttaqi, and D. Sutanto, "An approach for online assessment of rooftop solar PV impacts on low-voltage distribution networks," *IEEE Trans. Sustain. Energy*, vol. 5, no. 2, pp. 663–672, April 2014.
- [14] W. Shi, X. Xie, C.-C. Chu, and R. Gadh, "Distributed optimal energy management in microgrids," *IEEE Trans. Smart Grid*, vol. 6, no. 3, pp. 1137–1146, May 2015.
- [15] R. T. Sauer, K.J. and C. Hansen, "Modeling the irradiance and temperature dependence of photovoltaic modules in PVsyst," *IEEE Journal of Photovoltaics*, vol. 5, no. 1, pp. 152–158, Jan 2015.
- [16] T. K. R. Chenni, M. Makhlof and A. Bouzid, "A detailed modeling method for photovoltaic cells," *J Energy*, vol. 32, no. 9, pp. 1724 – 1730, 2007.
- [17] A. Mohammed, J. Pasupuleti, T. Khatib, and W. Elmenreich, "A review of process and operational system control of hybrid photovoltaic/diesel generator systems," *J Renew. and Sustain. Energy Rev.*, vol. 44, pp. 436–446, 2015.
- [18] A. M. Ameen, J. Pasupuleti, and T. Khatib, "Simplified performance models of photovoltaic/diesel generator/battery system considering typical control strategies," *J Energy Convers. and Manag.*, vol. 99, pp. 313–325, 2015.